

Electrokinetic origin of swirling flow on nanoscale interface

Shuangshuang Meng,^{1,#} Yu Han,^{1,#} Wei Zhao,^{1,*} Yueqiang Zhu,¹ Chen Zhang,¹ Xiaoqiang Feng,¹ Ce Zhang,^{1,*} Duyang Zang,²
Guangyin Jing,³ Kaige Wang,^{1,*}

¹ State Key Laboratory of Photon-Technology in Western China Energy, International Collaborative Center on Photoelectric Technology and Nano Functional Materials, Institute of Photonics & Photon Technology, Northwest University, Xi'an 710127, China

² School of Physical Science and Technology, Northwestern Polytechnical University, Xi'an 710129, P. R. China

³ School of Physics, Northwest University, Xi'an 710127, China

* Corresponding authors: zwbayern@nwu.edu.cn; zhangece.univ@gmail.com; wangkg@nwu.edu.cn

These authors have equal contributions to this investigation

Abstract The zeta (ζ) potential is a pivotal metric for characterizing the electric field topology within an electric double layer—an important phenomenon on phase interface. It underpins critical processes in diverse realms such as chemistry, biomedical engineering, and micro/nanofluidics. Yet, local measurement of ζ potential at the interface has historically presented challenges, leading researchers to simplify a chemically homogenized surface with a uniform ζ potential. In the current investigation, we present evidence that, within a microchannel, the spatial distribution of ζ potential across a chemically homogeneous solid-liquid interface can become two-dimensional (2D) under an imposed flow regime, as disclosed by a state-of-art fluorescence photobleaching electrochemistry analyzer (FLEA) technique. The ζ potential's propensity to become increasingly negative downstream, presents an approximately symmetric, V-shaped pattern in the spanwise orientation. Intriguingly, and of notable significance to chemistry and engineering, this 2D ζ potential framework was found to electrokinetically induce swirling flows in tens of nanometers, aligning with the streamwise axis, bearing a remarkable resemblance to the well-documented hairpin vortices in turbulent boundary layers. Our findings gesture towards a novel perspective on the genesis of vortex structures in nanoscale. Additionally, the FLEA technique emerges as a potent tool for discerning ζ potential at a local scale with high resolution, potentially accelerating the evolution and applications of novel surface material.

The electric double layer (EDL) epitomizes an essential physical paradigm omnipresent at solid-liquid interfaces, performing a pivotal role in mediating interfacial transport phenomena within multiple systems, spanning electrochemical, micro/nanofluidic, and biomedical disciplines¹. Elucidation of the electric potential landscape and dynamics of the EDL is essential for a comprehensive understanding of interface reactions², enabling self-assembly of materials^{3,4}, protein-DNA recognition⁵, and even altering the structure of solvent⁶⁻⁸ in proximity to solid interfaces.

The structure of EDL can be highly complex, as the liquid circumstance is ordinarily non-static and the solid part is non-uniform. Just as the wind blows across the desert, creating sand dunes, in turn affecting the atmospheric airflow near the surface. When water flows across an interface, it should also generate charge accumulation, thereby influencing the flow of water near the interface. ζ potential, which is crucial to characterize the electric potential landscape of the EDL, should be inherent two-dimensional (2D) on solid-liquid interface.

Unfortunately, probing local ζ potential is highly challenging⁹ and requires a novel diagnostic apparatus^{10,11}. Most of the current techniques, e.g. light scattering method¹² and streaming current method¹³, can only measure the overall ζ potential on particles and solid surfaces. Although Lis et al.¹⁴ and Ober et al.¹⁵ have demonstrated flow can induce perturbations in the surface charge density, thereby modulating the ζ potential on calcium fluoride and fused silica substrates, by vibrational sum frequency generation spectroscopy (v-SFG). A comprehensive picture of how flow interplays with surface charge and ζ potential distribution is still lacking.

In this investigation, we utilized a novel fluorescence photobleaching electrochemistry analyzer (FLEA) technique and present experimental evidence of a 2D distribution of ζ potential induced on a chemically uniform and insulated surface. For the first time, we demonstrate that streamwise vortices, which are broadly existed in boundary flows and play important roles, can be originated at tens of nanometers away from the

solid-liquid interface, according to the 2D ζ potential. This result could be important for understanding interfacial reaction progress in a non-static system and leading to the development of novel approaches for flow control.

FLEA provides high spatial resolution (~ 180 nm) to measure of local ζ potential on an interface, on the basis of laser induced fluorescent photobleaching¹⁶⁻²². By measuring the oscillating velocity (v_{rms}) of electroosmotic flow (EOF) and the corresponding driven AC electric field (E_{rms}), ζ potential can be determined by Helmholtz-Smoluchowski relation in low-frequency oscillating EOF^{23,24}, as

$$\zeta = \frac{\eta}{\epsilon_0 \epsilon_r} \frac{v_{rms}}{E_{rms}} \quad (1)$$

where ϵ_r and ϵ_0 are the relative and vacuum permittivity, η is dynamic viscosity of solution.

The FLEA system is constructed on the foundation of an internally developed confocal microscope, incorporating a 100X oil immersion objective (Olympus Plan Apo NA1.4) and a 405 nm continuous wave laser. Its spatial resolution is approximately 180 nm in the lateral direction and 800 nm in the axial direction. Accompanied with a nano-resolution piezo stage (P-611.3SF, Physik Instrumente), the detection position can be accurately located in three dimensions to cover the shear plane of EDL (Fig. 1) where the v_{rms} reaches maximum. During the experimental procedure, the ζ potential is investigated on the surface of a glass cover slide, assembled in a microchip fabricated through a layer-by-layer protocol (see Supplementary Materials). Furthermore, a laminar basic flow with a bulk flow Reynolds number of $Re = \langle U \rangle D \rho_f / \eta = 1.13$ (where D is hydraulic diameter and ρ_f is fluid density) has been implemented during FLEA measurement, revealing comprehensive insights into the velocity (U) of basic flow on ζ potential distribution.

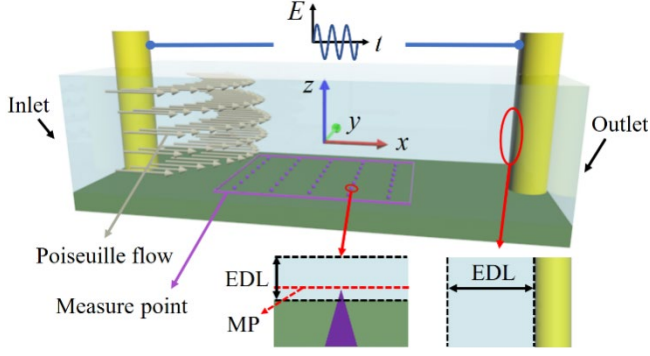


Figure 1 | Schematic diagram of microchip. The microchannel is $L = 5$ mm long, $w = 500 \mu\text{m}$ wide and $h = 90 \mu\text{m}$ high. Two platinum electrodes are placed in the inlet and outlet to generate oscillating EOF driven by AC electric field. ζ potential is directly measured through oscillating velocity on the shear plane in EDL of solid-liquid interface at the measurement point (MP). A basic pressure-driven flow has been applied in x -directions, with y -directions and z -directions being spanwise and vertical directions respectively. The working fluid is Coumarin 102 (C102) aqueous solution of different electric conductivity and pH values. The thickness of EDL can be evaluated by Debye length which is $\lambda = 11$ nm.

Fig. 2 demonstrates the impact of external flow on the ζ potential at different pH values, bulk electric conductivity, and flow velocities. The results show that the ζ potential becomes increasingly negative along the streamwise direction of flow for a broad range of pH values (Fig. 2a), indicating an accumulation of surface charge on the solid-liquid interface,

as theoretically predicted by Werkhoven et al.²⁵. At pH=7, there is an exception, which suggests a different surface charge behavior close to the dissociation constant (i.e. pK) of the solution. Moreover, the ζ potential increases with the bulk electric conductivity (Fig. 2b) of the solution and the flow velocity (Fig. 2e). These findings reveal the complex interplay between external flow and surface charge density in micro/nanofluidics.

An intriguing observation that emerged from our study is that the ζ potential does not only vary with the streamwise position, but displays a marked spanwise variation (Fig. 2d,e). Specifically, the ζ potential is consistently more negative at the center of the microchannel and exhibits fewer negative values near the side walls as a result of the higher flow velocity (Fig. 2c). Thus, even in the context of a laminar basic flow, the ζ potential displays an intrinsic 2D distribution (Fig. 2f) on a chemically uniform surface. Given that the microchannel is significantly longer than the measurement region, it is impractical for the ζ potential to remain infinitely large downstream. Consequently, the ζ potential either asymptotically approaches a saturation value, or exhibits oscillatory ripple structures akin to sand surfaces in a desert.

The 2D distribution of ζ potential, which is induced by flow, can lead to a 3D distribution of electric potential (φ) near the solid-liquid interface. According to the Poisson-Boltzmann theory ($\varphi(x, y, z) = (4k_B T / e z_i) \tanh^{-1}[\tanh(e z_i \zeta / 4k_B T) \exp(-z/\lambda)]$), this distribution of electric potential can result in an electric volume force ($\vec{F}_e = \rho_e \vec{E} = \varepsilon \nabla^2 \varphi \nabla \varphi$) that is primarily in the negative z direction and is larger near the solid-liquid interface (Fig. 3a). This force, even though primarily balanced by pressure gradient (Extended Data Fig.5), drives the flow upward until a certain distance ($z^* \approx 1$, approximately one Debye length) and then bends downstream (Fig. 3b).

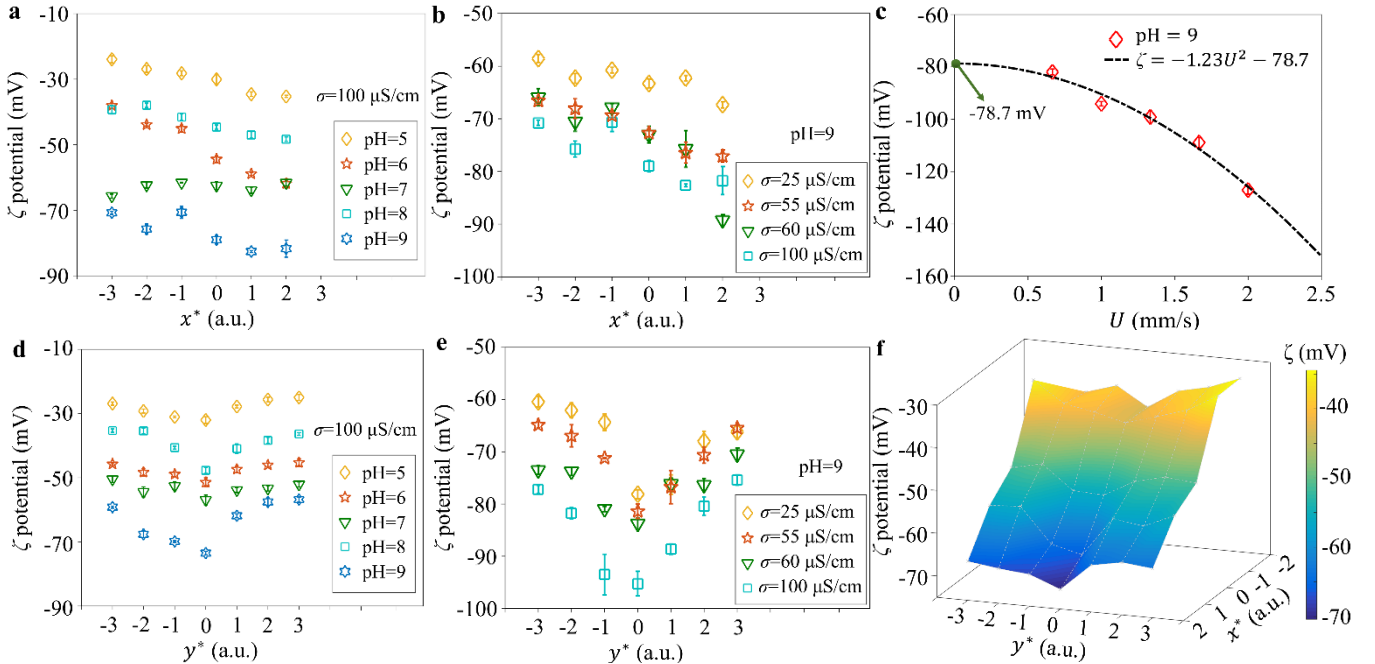


Figure 2 | Distribution of ζ potential induced by external flow. **a, b,** ζ potential distribution along the flow direction at $y = y^*w$, i.e., the centerline. All the $\zeta \sim x$ plots declined towards downstream indicates a decreasing of ζ potential along streamwise direction. **d, e,** ζ potential distribution along spanwise direction at $x = x^*L$. The minimum ζ potential locates at the center of microchannel and ζ potential is approximately symmetric in spanwise distribution. **a, d,** $\sigma = 100 \mu\text{S/cm}$, different pH value. As pH value is increased, ζ potential is decreased and more negative. **b, e,** pH=9, different conductivity. As σ is increased, ζ potential is decreased and more negative. **c,** ζ potential vs flow velocity U (where $U = |\vec{u}|$) measured at the centerline of microchannel, where $\sigma = 100 \mu\text{S/cm}$ and pH=9. ζ potential is always more negative at higher U . This is consistent with the findings of Ober et al.¹⁵ that surface charge density (which monotonically increases with ζ potential) increases with flow rate. **f,** 2D distribution of ζ potential induced by flow on the chemically uniform surface, where $\sigma = 100 \mu\text{S/cm}$ and pH=9.

The numerical simulation conducted using COMSOL Multiphysics software supports these findings, showing that the velocity distribution of the flow is highly nonuniform and asymmetric due to the influence of the 2D distribution of ζ potential. The flow pattern is different from what would be expected without considering this distribution (Fig. 3c). The theoretical predictions (see the Theory part in supplementary materials) suggest that when the 2D distribution of ζ potential is nonuniform, the electric volume force near the EDL can be nonconservative or rotational. The curl of the force, $\vec{T} = \nabla \times \vec{F}_e$, which is the driving term of the vorticity equation, can be non-zero. As a result, a vortical flow could be generated adjacent to the EDL at the nanoscale.

Through numerical simulations, we do observe vortex structures (Fig. 3d) within a region of $z^* < 4$, i.e. approximately 44 nm close to the insulated wall, which is the smallest scale ever observed in fluids. The vertical sizes of these vortex structures are only about ten times larger than the surface roughness of the cover slide. They are also 2-3 orders smaller than Kolmogorov scale in regular fluids, and the vortices in superconductors²⁶ and quantum fluids²⁷.

An interesting observation is that when the distance from the insulated wall exceeds 22 nm, i.e. $z^* > 2$, the vortex structures become dominant in the streamwise direction, as can be inferred from Fig. 3d and e from Ω_x which is the streamwise component of vorticity $\vec{\Omega} = \nabla \times \vec{u}$. These vortex structures exhibit similarities to hairpin vortices, which are well-known coherent vortex structures in turbulent boundary layers. This similarity

suggests that the dynamics of EDL at the nanoscale may be involved in the origination of these vortex structures. It is worth noting that the vortex structures are not influenced by any external electric field but rather by the internal electric field within the EDL, which is determined by the 2D distribution of ζ potential. These vortex structures are advected along the mean flow field, resulting in a helical flow pattern, as shown by the helicity in Fig. 3f, and leading to preserved influence on the interfacial flow. This observation of vortical flow phenomena adjacent to the EDL, driven by the nonuniform distribution of ζ potential, is a novel and previously unobserved and unpredicted result.

The experimental investigation discussed in the article has revealed a 2D distribution of ζ potential induced by flow, which holds great potential for advancing various fields such as chemical engineering, electrochemistry, biomedical engineering, and micro/nano fluidics devices. The utilization of cutting-edge techniques like fluorescence photobleaching electrochemistry analyzer enables local and high-resolution measurement of ζ potential, thereby offering a new approach for electrochemical analysis and surface characterization of artificially designed metamaterials. These findings can also shed light on current observations in interfacial sciences, such as the chaotic electroosmotic flow observed on chemically uniform and insulated surfaces. Overall, this breakthrough has the capacity to greatly advance the development of novel and complex chemical and biomedical materials for broad applications.

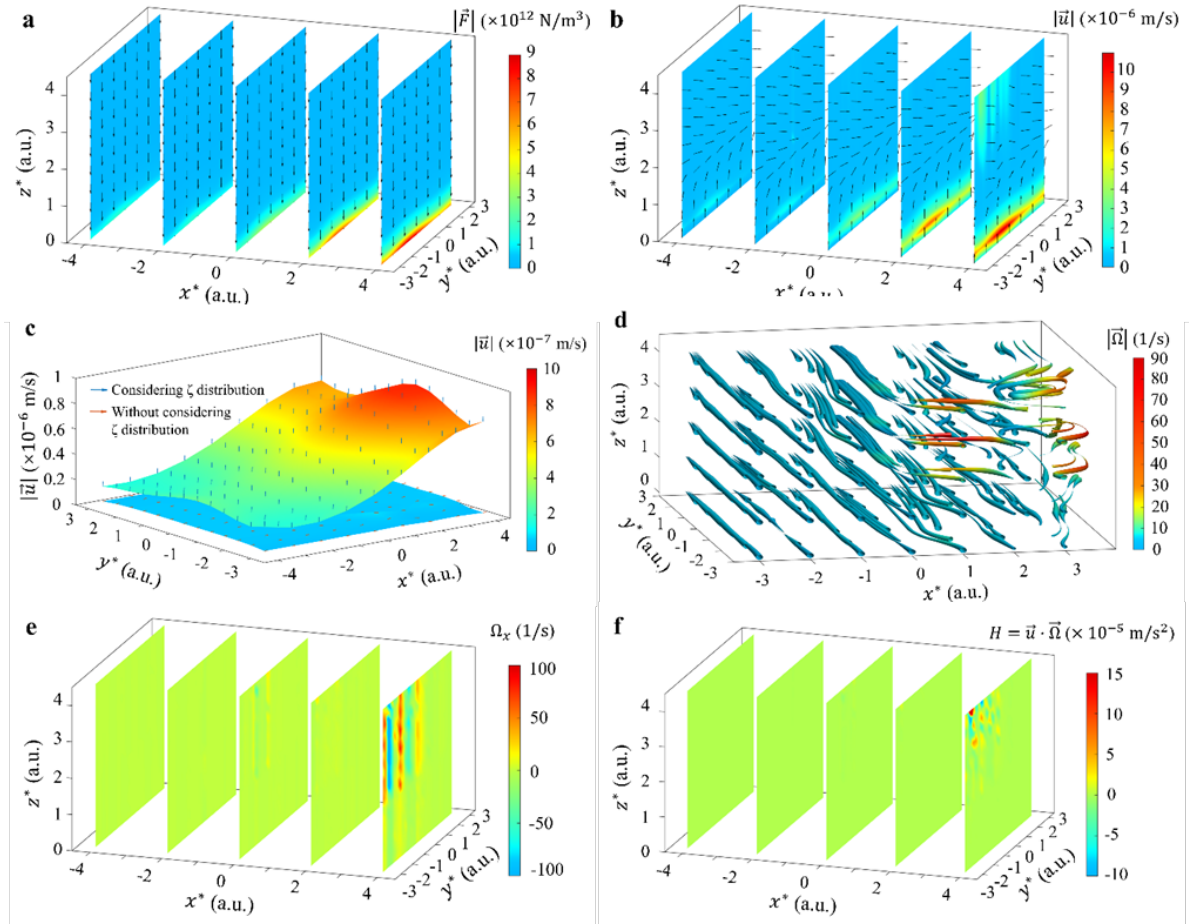


Figure 3 | a, Electric volume force \vec{F}_e generated according to the 2D distribution of ζ potential induced by laminar basic flow. \vec{F}_e has a larger z-directional components and towards the bottom wall. Its magnitude increases along streamwise direction, and exhibits asymmetry in spanwise. b, The 3D distribution of fluid velocity \vec{u} . c, the 2D velocity distribution of flow considering and without considering ζ potential distribution at $z^* = 1$, showing the influence of 2D distribution of ζ potential. d, Stream tube diagram of vorticity $\vec{\Omega} = \nabla \times \vec{u}$. e, 3D distribution of Ω_x , which is the vorticity of velocity component u . f, 3D distribution of helicity $H = \vec{u} \cdot \vec{\Omega}$. All of these results are simulated by COMSOL Multiphysics software.

Acknowledgement The investigation is supported by National Natural Science Foundation No. 51927804.

Reference

- 1 Sparreboom, W., Berg, A. & Eijkel, J. C. Principles and applications of nanofluidic transport. *Nature Nanotechnology* **4**, 713-720 (2009).
- 2 Jr., G. E. B. *et al.* Metal Oxide Surfaces and Their Interactions with Aqueous Solutions and Microbial Organisms. *Chemical Reviews* **99**, 77-174 (1999).
- 3 Shi, S. *et al.* Self-Assembly of MXene-Surfactants at Liquid-Liquid Interfaces: From Structured Liquids to 3D Aerogels. *Angewandte Chemie* **58**, 18171-18176 (2019).
- 4 Zhang, S. *et al.* Engineering Biomolecular Self-Assembly at Solid-Liquid Interfaces. *Advanced Materials* **33**, 1905784 (2021).
- 5 Rohs, R. *et al.* The role of DNA shape in protein-DNA recognition. *Nature* **461**, 1248-1253 (2009).
- 6 Du, Q., Freysz, E. & Shen, Y. R. Vibrational Spectra of Water Molecules at Quartz/Water Interfaces. *Physical Review Letters* **72**, 238 (1994).
- 7 Wernet, P. *et al.* The Structure of the First Coordination Shell in Liquid Water. *Science* **304**, 995-999 (2004).
- 8 Jena, K. C. & Hore, D. K. Water structure at solid surfaces and its implications for biomolecule adsorption. *Physical Chemistry Chemical Physics* **12**, 14383-14404 (2010).
- 9 Schaefer, J., Gonella, G., Bonn, M. & Backus, E. H. G. Surface-specific vibrational spectroscopy of the water/silica interface: screening and interference. *Physical Chemistry Chemical Physics* **19**, 16875-16880 (2017).
- 10 Delgado, A. V., González-Caballero, F., Hunter, R. J., Koopal, L. K. & Lyklema, J. Measurement and interpretation of electrokinetic phenomena. *Journal of Colloid and Interface Science* **309**, 194-224 (2007).
- 11 Arjmandi, N., Roy, W. V., Lagae, L. & Borghs, G. Measuring the Electric Charge and Zeta Potential of Nanometer Sized Objects Using Pyramidal-Shaped Nanopores. *Analytical Chemistry* **84**, 8490-8496 (2012).
- 12 Kaszuba, M., Corbett, J., Watson, F. M. & Jones, A. High-concentration zeta potential measurements using light-scattering techniques. *Philosophical Transactions of The Royal Society A* **368**, 4439-4451 (2010).
- 13 Wang, J., Hu, H., Guan, W. & Li, H. Electrokinetic experimental study on saturated rock samples: zeta potential and surface conductance. *Geophysical Journal International* **201**, 869-877 (2015).
- 14 Lis, D., Backus, E. H. G., Hunger, J., Parekh, S. H. & Bonn, M. Liquid flow along a solid surface reversibly alters interfacial chemistry. *Science* **344**, 1138-1142 (2014).
- 15 Ober, P. *et al.* Liquid flow reversibly creates a macroscopic surface charge gradient. *Nature Communications* **12**, 4102 (2021).
- 16 Wang, G. R. Laser induced fluorescence photobleaching anemometer for microfluidic devices. *Lab on a Chip* **5**, 450-456 (2005).
- 17 Zhao, W. *et al.* Study of Oscillating Electroosmotic Flows with High Temporal and Spatial Resolution. *Analytical Chemistry* **90**, 1652-1659 (2018).
- 18 Hu, Z. Y. *et al.* Transition from periodic to chaotic AC electroosmotic flows near electric double layer. *AIChE Journal* **67**, 17148-17160 (2021).
- 19 Hu, Z. *et al.* Onset of Nonlinear Electroosmotic Flow under an AC Electric Field. *Analytical Chemistry* **94**, 17913-17921 (2022).
- 20 Wang, G., Yang, F. & Zhao, W. There can be turbulence in microfluidics at low Reynolds number. *Lab on a Chip* **14**, 1452 - 1458 (2014).
- 21 Wang, G., Yang, F. & Zhao, W. Microelectrokinetic turbulence in microfluidics at low Reynolds number. *Phys Rev E* **93**, 013106 (2016).
- 22 Kuang, C., Yang, F., Zhao, W. & Wang, G. Study of the Rise Time in Electroosmotic Flow within a Microcapillary. *Anal. Chem.* **81**, 6590-6595 (2009).
- 23 Ohshima, H. Approximate Analytic Expression for the Electrophoretic Mobility of Moderately Charged Cylindrical Colloidal Particles. *Langmuir* **31**, 13633-13638 (2015).
- 24 Sze, A., Erickson, D., Ren, L. & Li, D. Zeta-potential measurement using the Smoluchowski equation and the slope of the current-time relationship in electroosmotic flow. *Journal of Colloid and Interface Science* **261**, 402-410 (2003).
- 25 Werkhoven, B. L., Everts, J. C., Samin, S. & van Roij, R. Flow-Induced Surface Charge Heterogeneity in Electrokinetics due to Stern-Layer Conductance Coupled to Reaction Kinetics. *Physical Review Letters* **120**, 264502-264507 (2018).
- 26 Ge, J.-Y. *et al.* Nanoscale assembly of superconducting vortices with scanning tunnelling microscope tip. *Nature Communications* **7**, 13880 (2016).
- 27 Dominici, L. *et al.* Interactions and scattering of quantum vortices in a polariton fluid. *Nature Communications* **9**, 1467 (2018).